Earth, Planets and Space

FULL PAPER

Open Access

Response of aurora candidates in the Chinese official histories to the space climate during 511–1876

Po-Han Lee[1] and Jann-Yenq Liu[1,2,3*]

Abstract

Continuous observations at specified locations and chronicling of astronomical phenomena provide a good opportunity to study ancient space weather. There are 248 white, 125 red, and 44 blue color aurora-like descriptions, also known as aurora candidates, recorded in Chinese official historical records during the 1365-year period of 511–1876. Qualitative descriptions of the color, location, and appearance time of these candidates are quantitatively denoted. The red, white, and blue aurora candidates occurred most frequently 34% in autumn, 32% in summer, and 49% in summer, respectively. The white and red aurora as well as the overall candidates tend to appear during high solar activity periods. By contrast, the blue candidates frequently occur during low solar activity periods. Statistical results with 90% confidence intervals further show that the relationship between solar activities and overall/red (white/blue) aurora candidates is significant (insignificant). The red aurora candidates that frequently occurred in autumn during the periods of high solar activity agree well with those of low/middle latitude auroras, while the white aurora candidates might be confounded by noctilucent clouds or other atmospheric optical events, such as airglows, moon halo, etc. The study of ancient space weather/climate based on historical records shows that aurora occurrences are related to solar activities, and in particular, red auroras frequently appear in low/middle latitudes during high solar activity periods.

Keywords Aurora, Historical record, Confident interval

*Correspondence:
Jann-Yenq Liu
jyliu@jupiter.ss.ncu.edu.tw
Full list of author information is available at the end of the article

Graphical Abstract

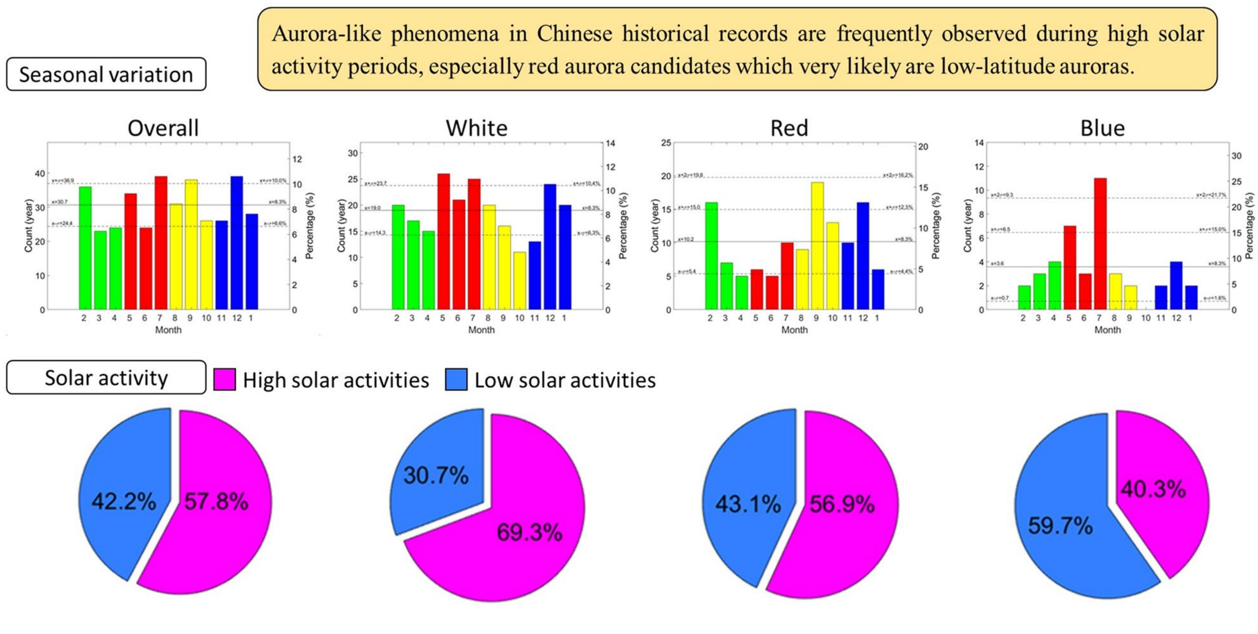

Introduction

Aurora, named after the Roman goddess of dawn, is a remarkable astronomical phenomenon caused by collisions between fast-precipitating electrons from space and the gases in Earth's upper atmosphere (Siscoe 1978; Kázmér and Timár 2016). When these gases are excited by the collisions, they return to their normal state by emitting electromagnetic waves at several specific frequencies, resulting in vibrant and colorful auroras (Gupta 2020). Aurora sightings have been most common in the countries within the auroral oval, which traces a path across central Alaska and Canada, Greenland, as well as northern Scandinavia and Russia in 1983–2016 (Zossi et al. 2021). They report that auroras can even be observed in middle latitudes, such as northern China, Japan, Korea, England, France, Italy, and elsewhere during high solar activity periods. On the other hand, auroras have been observed and recorded throughout history. Various lists of ancient observations of auroras in China (Schove 1979; Keimatsu 1976; Yau et al. 1995; Hayakawa et al. 2015, 2017a; Kawamaru et al. 2016; Tamazawa et al. 2017), Japan (Matsushita 1956; Keimatsu 1976; Nakazawa et al. 2004; Shiokawa et al. 2005; Hayakawa et al. 2017b), and Korea (Keimatsu 1976; Lee et al. 2004; Wang et al. 2021a) have been published. Willis and Stephenson (2000) compare observations of aurora-like descriptions which display at more than one site in East Asia on the same night. The good level of agreement between the detailed auroral descriptions recorded in the different oriental histories provides virtually incontrovertible proof that auroral displays occurred on these special occasions. These records provide a conservative estimate of the intensity of magnetic storms and help reconstruct ancient magnetic fields or space weather (Hattori et al. 2019; Wang et al. 2021b). Notably, the Carrington event (Carrington 1859), the historically largest geomagnetic sudden commencement, was also recorded as a stunning aurora in historical books from all around the world (Loomis 1860; Kimball 1960; Hayakawa et al. 2016, 2018).

Auroral emissions observed in mid- and low-latitude regions, usually at geomagnetic latitudes below 50 degrees, are commonly referred to as "low-latitude auroras" or "mid-latitude auroras" (Tinsley et al. 1984; Rassoul et al. 1993; Mendillo and Wroten 2019). The first recorded aurora-like descriptions were found in an ancient Chinese book, Bamboo Annals (竹書紀年: Zhúshū Jìnián), in the early tenth century BC (Before Christ) (Sluijs and Hayakawa 2022). Hayakawa et al. (2015) find that the records of luminous phenomena, especially aurora-like descriptions, observed at night are potentially those of auroras, and are termed "aurora candidates". Scientists (Hayakawa et al. 2015, 2017a;

Kawamaru et al. 2016; Tamazawa et al. 2017) collect the records of luminous phenomena observed at night in the Chinese official histories during 511–1912 and study the relationship between aurora candidates and the moon phase, as well as the observation of sunspots with the naked eye in each dynasty. Meanwhile, Hayakawa et al. (2017a) surveyed aurora candidates during 1261–1644 and found that the peaks of records are consistent with contemporary total solar irradiance (TSI). Abbott and Juhl (2016) examined the aurora candidates during 500–1770 and found that white aurora candidates are significantly more abundant during low solar activity periods, while red aurora candidates are the opposite. However, Tamazawa et al. (2017) investigated records of aurora candidates for the sixth–tenth century and show irrelevant to the long-term change in solar activity. To resolve the discrepancy, this paper integrates the data of Hayakawa et al. (2015, 2017a), Kawamaru et al. (2016), and Tamazawa et al. (2017) to statistically rigorously examine the relationship between aurora candidates and solar activities over a millennium scale during 511–1876 CE. Moreover, to have a better understanding of their connection to solar activity, seasonal variations of these ancient auroras are for the first time examined.

Materials and methods

Chinese astronomical records, which were compiled by trained experts in the field, are considered valuable scientific data among historical records worldwide (Keimatsu 1976; Hayakawa et al. 2015). The first volume of the twenty-five official dynastic histories, Shiji, completed around 94 BC during the Han dynasty, documents various astronomical phenomena, including auroras, sunspots, eclipses, and meteors (Sima 1961; Song, 1992). The consistent observations of these phenomena at specific locations, along with details about their movements, shapes, and colors, offer a unique opportunity to explore ancient Chinese environments and even space weather (Keimatsu 1976). Hayakawa et al. (2015, 2017a), Kawamaru et al. (2016), and Tamazawa et al. (2017) study the relationship between auroras and the moon phase, as well as the observation of sunspots with the naked eye in each dynasty. Comprehensive datasets of aurora records in ancient China have been published by the above articles and are available in Database of Aurora/Sunspot in Chronicle (2015). Seven datasets summarize the observations of auroras in the Suí dynasty (511–619 CE), Táng dynasty (618–907 CE), Five Dynasties and Ten Kingdoms (907–960 CE), Sòng dynasty (960–1279 CE), Yuán dynasty (1234–1368 CE), Míng dynasty (1368–1644 CE), and Qīng dynasty (1616–1912 CE). Each dataset provides the following information about aurora candidates: year, month, date, color, description (describing as vapor, cloud, or both), direction, length, counts, place, notes (i.e., near the moon, until morning, covered half the sky, etc.), moon phase, bibliography, and its original sentence. After combining all datasets, a total of 391 aurora events were identified between 511 and 1912 CE. To rigorously conduct the statistical analysis, the data are converted into the Boolean format by assigning "1" to years with auroras and "0" to those without. Additionally, if an event was recorded in multiple historical records or occurred in overlapping years, months, or locations, it was counted only once to avoid double counting. Moreover, if there is more than one color denoted in the same event, it would be counted once in each color separately. Overall, there were 215 event years (i.e., 1187 non-event years) in 391 aurora candidates, 145 event years (i.e., 1257 non-event years) in 248 white candidates, 74 event years (i.e., 1328 non-event years) in 125 red candidates, 31 event years (i.e., 1371 non-event years) in 44 blue candidates, as well as 31 event years (i.e., 1371 non-event years) in 32 candidates of other colors (Fig. 1).

Solar activity is known to vary over time, with periods of high and low activity occurring throughout history. In this paper, the classification of the periods into solar minimums is based on delta ^{14}C variations (Pang and Yau 2002), sunspot number reconstructed by ^{14}C (Usoskin et al. 2007), and total solar irradiance reconstructed by ^{10}Be and ^{14}C (Steinhilber et al. 2009; Solanki and Krivova 2013). Seven distinct solar minimums that occurred between the years 462 and 1912 CE are under study. These minimums are known as the Fifth-Century Minimum (462–526 CE), Medieval Minimum (580–820 CE), Oort Minimum (980–1070 CE), Wolf Minimum (1280–1350 CE), Sporer Minimum (1410–1590 CE), Maunder Minimum (1645–1715 CE), and Dalton Minimum (1795–1825 CE) (Stuiver and Braziunas 1989; Pang and Yau 2002; Usoskin et al. 2003; Knudsen et al. 2009; Steinhilber et al. 2012; Liu et al. 2022). To better understand the impact of these periods on auroral activity, we defined the time between two adjacent minimums as a period of high solar activity (HSA) and the minimum itself as a period of low solar activity (LSA). This allowed us to classify the years between 462 and 1825 CE into seven LSA and six HSA periods, as shown in Fig. 1.

To investigate the link between solar activities and aurora candidates, Fig. 2 depicts the proportions of aurora candidates during HSA and LSA calculated by dividing the aurora year counts by the year counts of the respective period. However, the proportion of the first LSA, which began in 462 CE, may be unreliable since the dataset only records observations after 511 CE. Thus, the proportion of the first LSA period is excluded from the subsequent analysis related to solar activities. To ensure the validity of our findings and not solely rely on

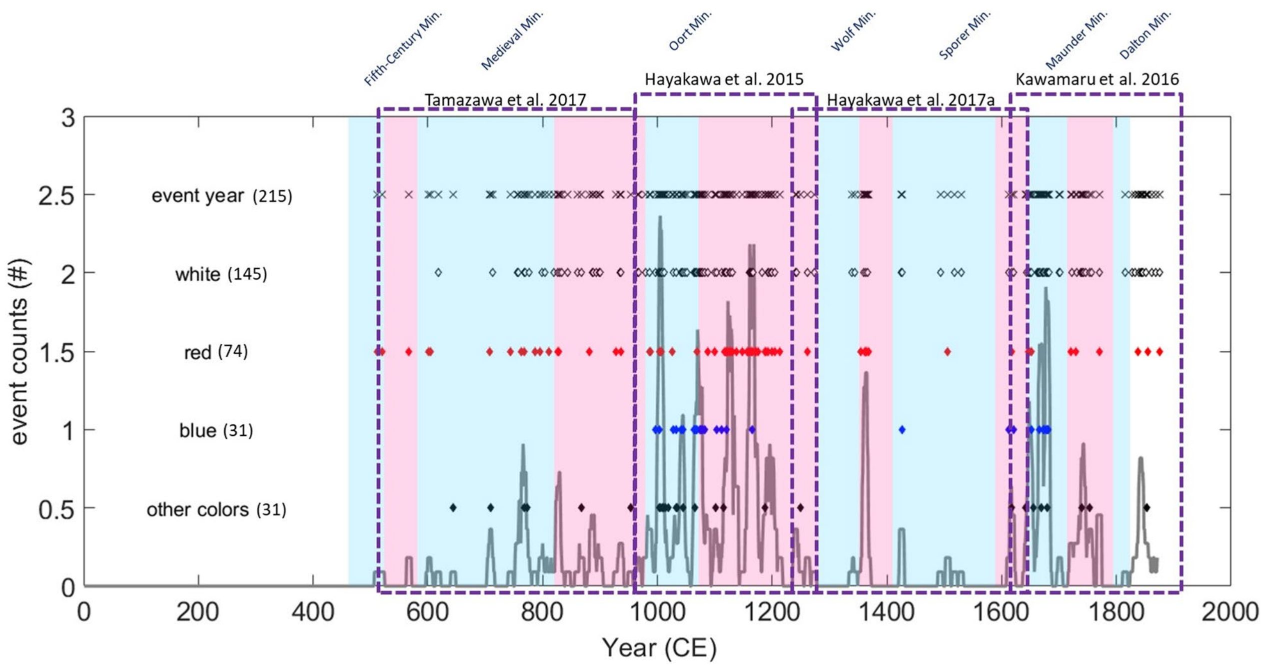

Fig. 1 Years and the 10-year moving average curve of 215 aurora candidates in China during 511–1876 CE. There are 7 solar minimums, low solar activities (LSA; blue bars), and 6 high solar activities (HSA; red bars). Years of the aurora candidates in all colors (cross symbols) as well as that in white (diamond symbols), red (red diamond symbols), blue (blue diamond symbols), and the other colors (black diamond symbols) are denoted

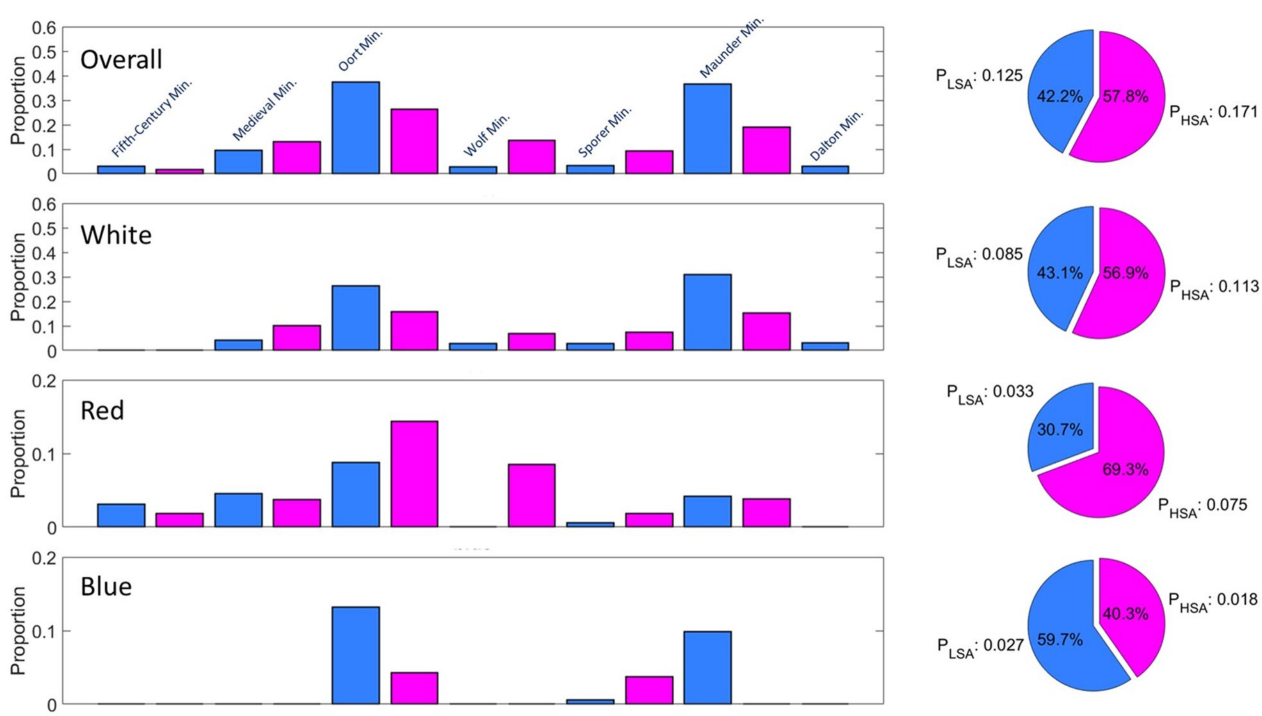

Fig. 2 Proportions of the aurora candidates in LSA and HSA periods. Overall, white, red, and blue in each solar activity period (bar chart on the left), and those during the whole periods (pie chart on the right). The proportion is computed by aurora year counts divided by the year counts of the period. The proportions of LSA (P_{LSA}) and HSA (P_{HSA}) periods are denoted

comparing the proportions, the 90% confidence intervals (CIs) for the differences between the proportions in the HSA and LSA periods are then constructed (Agresti 1996). Let P_H (P_L) denote the proportions in the HSA (LSA) periods, and the critical value (CV) of the 90% CIs is 1.645. The true difference between the two proportions then could be given by,

$$\left[P_H - P_L - CV * \sqrt{\frac{P_H(1-P_H)}{N_H} + \frac{P_L(1-P_L)}{N_L}}, P_H - P_L + CV * \sqrt{\frac{P_H(1-P_H)}{N_H} + \frac{P_L(1-P_L)}{N_L}}\right]$$

Note that the numbers of years involved in the HSA and LSA periods (excluding the first LSA) are $N_H = 613$ and $N_L = 686$, respectively. The 90% CIs are given in Table 1.

Results and interpretation

Figure 2 displays the proportions of various color aurora candidates in each HSA and LSA period. The proportions yield very large counts in the Oort minimum and Maunder minimums together with their followed high solar activity period, and the proportion of the two minimums is respectively greater than their followed high solar activity period. However, for the entire study period, the proportions of aurora candidates are generally higher during the HSA period compared to the LSA period, except for blue aurora candidates, which yield an opposite trend. Table 1 depicts that when considering overall aurora candidates, the proportion during HSA periods ($\boldsymbol{P_H}$=0.171) is higher than during LSA periods ($\boldsymbol{P_L}$=0.134) with a corresponding 90% CI of [0.004, 0.070]. In the case of white aurora candidates, the proportion is higher during the HSA period ($\boldsymbol{P_H}$=0.112) than during the LSA period ($\boldsymbol{P_L}$=0.093), while the 90% CI of [−0.009, 0.047] shows that this difference is not statistically significant. By contrast, the proportion of red aurora candidates is significantly high during the HSA period, with nearly 70% of red aurora candidates appearing during this period (Fig. 2). Table 1 reveals that the result is statistically significant under a 90% CI of [0.021, 0.062]. The result even meets the statistical significance of 95% CI of [0.017, 0.066]. It is surprising to see that no red aurora candidates occurred in the Wolf minimum and Dalton minimum. The blue aurora candidates are rarely observed and are simply recorded during two HSAs adjacent to three LSAs of the Oort, Sporer, and Maunder minimums. Even though a 90% CI of [−0.025, 0.003] does not meet the statistical significance, the blue aurora candidates appear more frequently during the LSA period ($\boldsymbol{P_L}$=0.029) than in the HSA period ($\boldsymbol{P_H}$=0.018). In short, the overall, white, and red aurora candidates occur more frequently during HSA periods, while the opposite is true for blue auroral candidates.

Table 1 Proportions and confidence interval of P_H–P_L during 511–1876

Aurora color	P_H	P_L	90% CI
Overall	0.171	0.134	[0.004, 0.070]
White	0.112	0.093	[−0.009, 0.047]
Red	0.075	0.034	[0.021, 0.062]
Blue	0.018	0.029	[−0.025, 0.003]

Figure 3 depicts the number and percentage of aurora candidates of all colors in each month. The percentage is computed by aurora candidates in each month divided by its total counts. It is found that 368 out of 391 events were denoted with their associated month information during 511–1876 CE. Although the original description of occurrence time is based on the Chinese lunar calendar, the database provided by Hayakawa et al. (2015, 2017a), Kawamaru et al. (2016), and Tamazawa et al. (2017) have converted it into the solar calendar in Common Era. To examine the seasonal variations of aurora candidates, we further classify seasons as Spring (February–April), Summer (May–July), Autumn (August–October), and Winter (November–January). Overall aurora candidates appear approximately equivalent in four seasons (spring: 23%, summer: 26%, autumn: 26%, winter: 25%). In fact, July in summer, September in autumn, and December in winter are greater than 10.0% (one standard deviation away from the mean) further supporting this idea. The highest occurrence of white aurora candidates is in summer, accounting for 32% of all observations. In contrast, the red aurora candidates occur the least frequently in summer, at 17%, but occur the most frequently in autumn, at 34%. The blue aurora candidates are most frequently observed during summer, accounting for 49% among the four seasons; the percentages in May and July are greater than one standard deviation of 15.0% and two standard deviations of 21.7%, respectively. These indicate that the blue aurora candidates significantly occur in summer. By contrast, no blue aurora candidates were observed in October.

Discussion and conclusion

Abbott and Juhl (2016) examined 1276 aurora candidates (66% of red, 20% of white, 6% of black, and 8% of other auroral colors) based on Chinese and Korean records

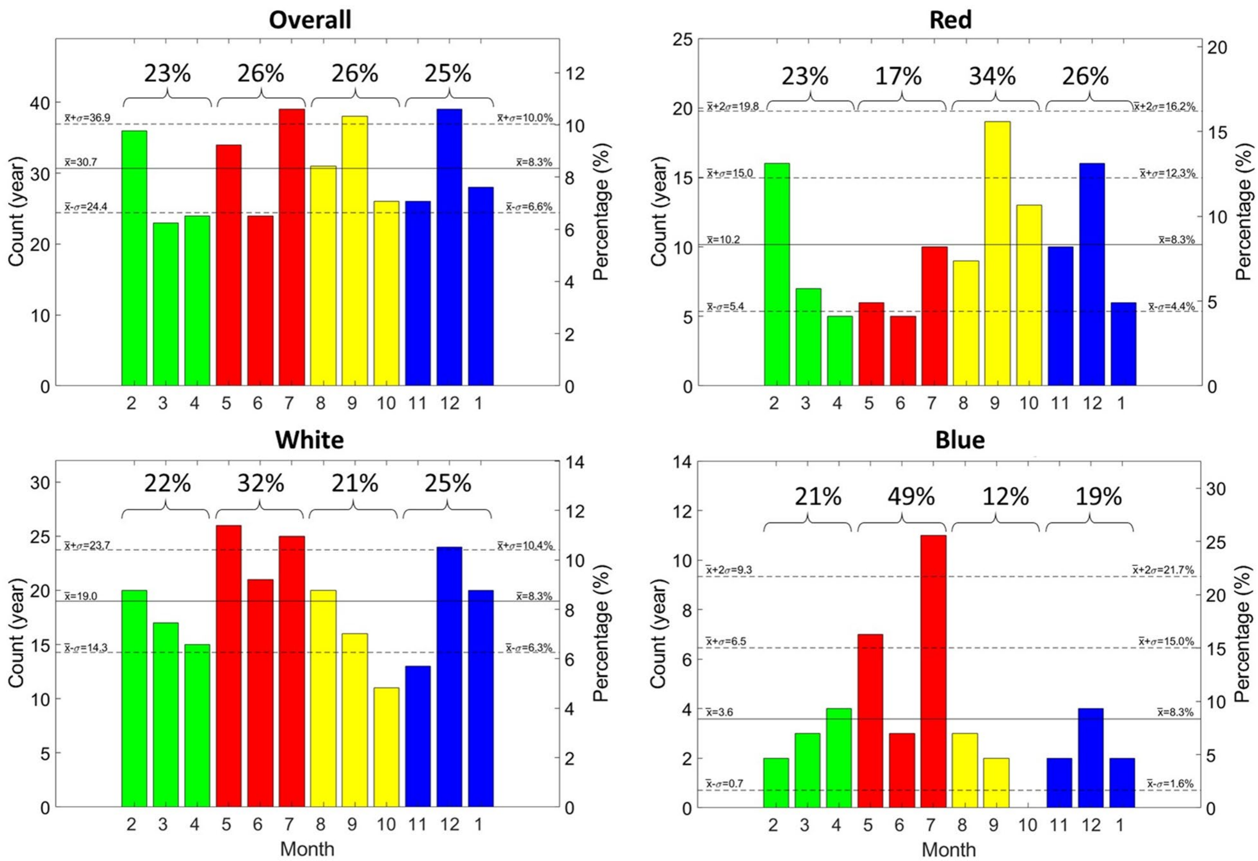

Fig. 3 Number and percentage of aurora candidates of various colors in each month and season. The percentage is computed by aurora year counts in each month divided by the year counts of study periods. The percentages of the four seasons and the mean value (x̄, solid lines) as well as it plus/minus the standard deviation (x̄±σ, dashed line) are denoted

from 500 to 1700 CE and applied bootstrapping techniques (Menke and Menke 2016) to the comparison of the aurora candidates and the ^{14}C production. To adequately compare the auroral data to the time series of estimated production of ^{14}C, they process the auroral data using the errors in the time series of ± 5 years (Usoskin and Kromer 2005), and program that adds each observation and its error in Gaussian to form a time series (Abbott and Isley 2002a, b; Isley and Abbott 1999, 2002). The findings of Abbott and Juhl (2016) align with our statistical results regarding red aurora candidates (Fig. 2), indicating that they occur more frequently during HSA periods. However, their results regarding white aurora candidates differ from our study. They found that white aurora candidates are more abundant during times of high ^{14}C production (i.e., lower solar activity) compared to periods of low ^{14}C production (i.e., higher solar activity). This discrepancy may be attributed to the use of the Korean dataset in their study. It is worth noting that our study does not assume any errors and provides independent results.

Hayakawa et al. (2017a) reported that the peaks of occurrence of aurora candidates are consistent with contemporary TSI, however, Tamazawa et al. (2017) found that those are irrelevant to the solar activity. Figure 1 displays that data in 581–959 CE (379 years) used by Tamazawa et al. (2017), 960–1279 CE (320 years) by Hayakawa et al. (2015), 1261–1644 CE (384 years) by Hayakawa et al. (2017a), and 1559–1912 CE (354 years) by Kawamaru et al. (2016) are relatively short, while the integrated data cover a period of 1365 years during 511–1876 CE. It can be seen that the previous studies simply cover 2 pairs of HSA and LSA periods that might not be suitable to investigate long-term variations associated with solar activities. We investigate the integrated data and find 90% confidence intervals (CIs) for the differences between auroras and solar activities over a millennium scale during 581–1876 CE. Figure 2 and Table 1 show that the aurora candidates occur more frequently during HSA periods, especially the red aurora candidate.

The statistical results of occurrences of aurora candidates in different solar activities and seasons show that aurora candidates of varying colors might originate from distinct mechanisms. The red aurora candidates are likely a type of red low-latitude aurora, specifically stable auroral red (SAR) arcs or type *d* auroras, which are produced by low-energy electrons (Collis et al. 1991; Rietveld et al. 1991; Rassoul et al. 1993). Note that most of the aurora candidates were recorded in the capitals of ancient Chinese dynasties (Keimatsu 1976; Hayakawa et al. 2015), which meet the criteria of "low-latitude auroras" or "mid-latitude auroras" and usually observed at geomagnetic latitudes below 50 degrees (Tinsley et al. 1984; Rassoul et al. 1993). The red aurora candidates significantly occurring more frequently during HSA is also consistent with observations of low-latitude auroras reported by scientists (Bellew and Silverman 1966; Abbott and Juhl 2016; Hayakawa et al. 2017b; Mendillo and Wroten 2019; Gupta 2020). Moreover, the occurrence rates that show SAR arcs to be least observed during summer months (Mendillo and Wroten 2019), which has good agreement with Fig. 3. To sum up, the red aurora candidates are most probable to be considered as low-latitude aurora.

Meanwhile, probably, some of the white aurora candidates recorded in the Chinese official histories could be attributed to atmospheric optical events such as moon halo, paraselene, sun dogs, parhelic circles, and 22° halo (Hayakawa et al. 2015; Kawamaru et al. 2016; Tamazawa et al. 2017). However, it is worth noting that these events do not show a clear association with solar activities or seasons. Interestingly, white aurora candidates were found to occur most frequently in the summer, which is similar to the occurrence of noctilucent clouds, since they are night-shining clouds consisting of ice crystals that form in a very high atmosphere and remain illuminated by the sun long after it has set at ground level (Gadsden and Schröder 1989). Note that, this phenomenon is frequently visible in mid-latitudes during the summer, and might be recorded as an aurora-like description in historical records. Gadsden and Schröder (1989) found that noctilucent clouds appear more frequently during LSA, while it has been known that auroras occur more frequently during HSA. It might be confounded effects that the CI of white aurora candidates crosses zero. Therefore, some of the white aurora candidates might be partially attributed to noctilucent clouds, which occur in a similar location and season to the white aurora candidates.

As for the blue aurora candidates, Gupta (2020) reported that molecular nitrogen and ionized molecular nitrogen produce visible light emissions, and radiate at a large number of wavelengths in both red and blue, especially 428 nm. Blue and purple emissions, typically at the lower edges of the "curtains", show up at the highest levels of solar activity. However, Fig. 2 and Table 1 show that the proportion of blue aurora candidates is oppositely higher during LSA periods, which suggests that the blue aurora candidates might be something else rather than auroras. In conclusion, this study examines the relationship between aurora candidates and solar activities, as well as their seasonal variations during the millennium scale of 511–1876 CE. The statistical results show that the red aurora candidates occur significantly frequently during high solar activities, which most likely are low-latitude auroras. The white aurora candidates are probably related to atmospheric optical events or noctilucent clouds.

Abbreviations

BC	Before Christ
CE	Common Era
LSA	Low solar activity
HSA	High solar activity
TSI	Total solar irradiance

Acknowledgements
The authors wish to thank Prof. Yuh-Ing Chen for the discussions of the statistical methods. This study is supported by the Taiwan National Science and Technology Council grant. This work was financially supported by the Center for Astronautical Physics and Engineering (CAPE) from the Featured Area Research Center program within the framework of Higher Education Sprout Project by the Ministry of Education (MOE) in Taiwan.

Author contributions
All authors read and approved the final manuscript.

Funding
This study is supported by the Taiwan National Science and Technology Council grant NSTC 112-2123-M-008-003. This work was financially supported by the Center for Astronautical Physics and Engineering (CAPE) from the Featured Area Research Center program within the framework of Higher Education Sprout Project by the Ministry of Education (MOE) in Taiwan.

Availability of data and materials
The datasets analyzed during the current study are available in the Database of Aurora/Sunspot in Chronicle, https://www.kwasan.kyoto-u.ac.jp/~palaeo/

Declarations

Ethics approval and consent to participate
Not applicable.

Consent for publication
Not applicable.

Competing interests
The authors declare that they have no competing interest.

Author details
[1]Department of Space Science and Engineering, National Central University, Taoyuan City, Taiwan. [2]Center for Astronautical Physics and Engineering, National Central University, Taoyuan City, Taiwan. [3]Center for Space and Remote Sensing Research, National Central University, Taoyuan City, Taiwan.

Received: 16 May 2023 Accepted: 5 September 2023
Published online: 13 September 2023

References

Abbott DH, Isley AE (2002a) Extraterrestrial influences on mantle plume activity. Earth Planet Sci Lett 205:53–62. https://doi.org/10.1016/S0012-821X(02)01013-0

Abbott DH, Isley AE (2002b) The intensity, occurrence and duration of superplume events and eras over geological time. J Geodyn 34(2002):265–307. https://doi.org/10.1016/S0264-3707(02)00024-8

Abbott D, Juhl R (2016) New historical records and relationships among 14C production rates, abundance and color of low latitude auroras and sunspot abundance. Adv Space Res 58(11):2181–2246. https://doi.org/10.1016/j.asr.2016.07.015

Agresti A (1996) An introduction to categorical data analysis. John Wiley, New York

Bellew W, Silverman S (1966) General behavior of 6300 Å [OI] at Sacramento Peak, New Mexico. Planet Space Sci 14(5):407–416. https://doi.org/10.1016/0032-0633(66)90012-2

Carrington RC (1859) Description of a singular appearance seen in the Sun on September 1, 1859. Mon Notices Royal Astron Soc 20:13–15. https://doi.org/10.1093/mnras/20.1.13

Collis P, Häggström L, Kaila K, Rietveld M (1991) Eiscat radar observations of enhanced incoherent scatter spectra; their relation to red aurora and field-aligned currents. Geophys Res Lett 18(6):1031–1034. https://doi.org/10.1029/91GL00848

Database of Aurora/Sunspot in Chronicle (2015) Kyoto University. https://www.kwasan.kyoto-u.ac.jp/~palaeo/. Accessed 20 July 2022

Gadsden M (1989) Schröder W (1989) Noctilucent Clouds. Springer-Verlag, Berlin Heidelberg

Gupta Swaroopa Rani N (2020) Review of Aurora borealis spectacular manifestations of solar wind and atmosphere. Int Res J Sci Eng 8(1):5–23

Hattori K, Hayakawa H, Ebihara Y (2019) Occurrence of great magnetic storms on 6–8 March 1582. Mon Notices Royal Astron Soc 487(3):3550–3559. https://doi.org/10.1093/mnras/stz1401

Hayakawa H, Tamazawa H, Kawamura AD, Isobe H (2015) Records of sunspot and aurora during CE 960–1279 in the Chinese chronicle of the Sòng dynasty. Earth Planet Sp 67:82. https://doi.org/10.1186/s40623-015-0250-y

Hayakawa H, Iwahashi K, Tamazawa H, Isobe H, Kataoka R, Ebihara Y, Miyahara H, Kawamura AD, Shibata K (2016) East Asian observations of low-latitude aurora during the Carrington magnetic storm. Publ Astron Soc Jpn 68(6):99. https://doi.org/10.1093/pasj/psw097

Hayakawa H, Tamazawa H, Ebihara Y, Miyahara H, Kawamura AD, Aoyama T, Isobe H (2017a) Records of sunspots and aurora candidates in the Chinese official histories of the Yuán and Míng dynasties during 1261–1644. Publ Astron Soc Jpn 69(4):65. https://doi.org/10.1093/pasj/psx045

Hayakawa H, Iwahashi K, Tamazawa H, Ebihara Y, Kawamura AD, Isobe H, Namiki K, Shibata K (2017b) Records of auroral candidates and sunspots in Rikkokushi, chronicles of ancient Japan from early 7th century to 887. Publ Astron Soc Jpn 69(6):86. https://doi.org/10.1093/pasj/psx087

Hayakawa H, Ebihara Y, Hand D, Hayakawa S, Kumar S, Mukherjee S, Veenadhari B (2018) Low-latitude aurorae during the extreme space weather events in 1859. Astrophys J. https://doi.org/10.3847/1538-4357/aae47c

Isley AE, Abbott DH (1999) Plume-related mafic volcanism and the deposition of banded iron-formation. J Geophys Res 104:15461–15477. https://doi.org/10.1029/1999JB900066

Isley AE, Abbott DH (2002) Implications of the temporal distribution of high Mg magmatism for mantle plume volcanism through time. J Geol 110(2002):141–158. https://doi.org/10.1086/338553

Kawamura AD, Hayakawa H, Tamazawa H, Miyahara H, Isobe H (2016) Aurora candidates from the chronicle of Qīng dynasty in several degrees of relevance. Publ Astron Soc Jpn 68(5):79. https://doi.org/10.1093/pasj/psw074

Kázmér M, Timár G (2016) The first scientific description of aurora borealis: the 10 September 1580 event in Transylvania, recorded by Marcello Squarcialupi. Geosci Lett 3:15. https://doi.org/10.1186/s40562-016-0047-2

Keimatsu M (1976) Chronology of aurorae and sunspots observed in China, Korea and Japan. Ann Sci Coll Lib Arts Kanazawa Univ 9:1–36

Kimball DS (1960) A Study of the Aurora of 1859. Scientific Report No. 6, NSF Grant No. Y/22.6/327, University of Alaska report UAG-R109, Fairbanks, Alaska, April 1960.

Knudsen MF, Riisager P, Jacobsen BH, Muscheler R, Snowball I, Seidenkrantz MS (2009) Taking the pulse of the sun during the Holocene by joint analysis of 14C and 10Be. Geophys Res Lett 36:L16701. https://doi.org/10.1029/2009GL039439

Lee EH, Ahn YS, Yang HJ, Chen KY (2004) The sunspot and auroral activity cycle derived from Korean historical records of the 11th–18th century. Sol Phys 224:373–386. https://doi.org/10.1007/s11207-005-5199-8

Liu JY, Chen YI, Lee PH, Haung CS, Fang TW (2022) Severe weather disasters in China linked to solar activity during 1–1825 Common Era. Geosci Lett 9:13. https://doi.org/10.1186/s40562-021-00210-x

Loomis E (1860) The great auroral exhibition of Aug. 28th to Sept. 4th, 1859. Am J Sci 2(90):339–361. https://doi.org/10.2475/ajs.s2-30.90.339

Matsushita S (1956) Ancient aurorae seen in Japan. J Geophys Res 61:297–302. https://doi.org/10.1029/jz061i002p00297-02

Mendillo M, Wroten J (2019) Modeling stable auroral red (SAR) arcs at geomagnetic conjugate points: Implications for hemispheric asymmetries in heat fluxes. J Geophys Res Space Phys 124:6330–6342. https://doi.org/10.1029/2019JA026904

Menke W, Menke J (2016) Environmental data analysis with MatLab. Elsevier Science and Technology Books, Cambridge, MA

Nakazawa Y, Okada T, Shiokawa K (2004) Understanding the "SEKKI" phenomena in Japanese historical literatures based on the modern science of low-latitude aurora. Earth Planet Space 56:e41–e44. https://doi.org/10.1186/BF03353323

Pang KD, Yau KK (2002) Ancient observations link changes in Sun's brightness and Earth's climate. Eos Trans AGU 83(43):481–490. https://doi.org/10.1029/2002EO000336

Rassoul HK, Rohrbaugh RP, Tinsley BA, Slater DW (1993) Spectrometric and photometric observations of low-latitude aurorae. J Geophys Res 98:7695–7709. https://doi.org/10.1029/92JA02269

Rietveld MT, Collis PN, St-Maurice JP (1991) Naturally enhanced ion acoustic waves in the auroral ionosphere observed with the EISCAT 933-MHz radar. J Geophys Res 96:19291–19305. https://doi.org/10.1029/91JA01188

Schove DJ (1979) Sunspot turning-points and aurorae since A.D. 1510. Sol Phys 63:423–432. https://doi.org/10.1007/BF00174546

Shiokawa K, Ogawa T, Kamide Y (2005) Low-latitude auroras observed in Japan: 1999–2004. J Geophys Res 110:A05202. https://doi.org/10.1029/2004JA010706

Sima Q (1961) Records of the grand history of China. Translated by Burton Waston. 2 vols. Columbia University Press, New York

Siscoe GL (1978) An historical footnote on the origin of "aurora borealis." Eos Trans Am Geophys Un 59(12):994. https://doi.org/10.1029/eo059i012p00994

Solanki S, Krivova N, Haigh J (2013) Solar irradiance variability and climate. Astronomische Nachrichten - ASTRON NACHR. https://doi.org/10.1146/annurev-astro-082812-141007

Song ZH (ed) (1992) Chronicle of Severe Natural Disaster and Anomaly in Ancient China (中國古代重大自然災害和異常年表總集in Chinese). Guangdong Education Press, Guangdong, pp 665. ISBN: 7540621036

Steinhilber F, Beer J, Fröhlich C (2009) Total solar irradiance during the Holocene. Geophys Res Lett 36:L19704. https://doi.org/10.1029/2009GL040142

Steinhilber F, Abreu JA, Beer J, Brunner I, Christl M, Fischer H, Heikkila U, Kubik PW, Mann M, McCracken KG, Miller H, Miyahara H, Oerter H, Wilhelms F (2012) 9,400 years of cosmic radiation and solar activity from ice cores and tree rings. Proc Natl Acad Sci 109(16):5967–5971. https://doi.org/10.1073/pnas.1118965109

Stuiver M, Braziunas T (1989) Atmospheric 14C and century-scale solar oscillations. Nature 338:405–408. https://doi.org/10.1038/338405a0

Tamazawa H, Kawamura AD, Hayakawa H, Tsukamoto A, Isobe H, Ebihara Y (2017) Records of sunspot and aurora activity during 581–959 CE in Chinese official histories concerning the periods of Suí, Táng, and the Five

Dynasties and Ten Kingdoms. Publ Astron Soc Jpn 69(2):22. https://doi.org/10.1093/pasj/psw132
Tinsley BA, Rohrbaugh RP, Rassoul H, Barker ES, Cochran AL, Cochran WD, Wills BJ, Wills DW, Slater D (1984) Spectral characteristics of two types of low latitude aurorae. Geophys Res Lett 11:572–575. https://doi.org/10.1029/GL011i006p00572
Usoskin IG, Kromer B (2005) Reconstruction of the ^{14}C production rate from measured relative abundance. Radiocarbon 47:31–37. https://doi.org/10.1017/S0033822200052176
Usoskin IG, Solanki SK, Schüssler M, Mursula K, Alanko K (2003) Millennium-scale sunspot number reconstruction: evidence for an unusually active Sun since the 1940s. Phys Rev Lett 91:211101. https://doi.org/10.1051/0004-6361:20077704
Usoskin IG, Solanki SK, Kovaltsov GA (2007) Grand minima and maxima of solar activity: new observational constraints. Astron Astrophys 471:301–309. https://doi.org/10.1051/0004-6361:20077704
van der Sluijs MA, Hayakawa H (2022) A candidate auroral report in the bamboo annals, indicating a possible extreme space weather event in the early 10th century BCE. Adv Space Res. https://doi.org/10.1016/j.asr.2022.0
Wang Y, Chen S, Xu K, Yan L, Yue X, He F, Wei Y (2021a) Ancient auroral records compiled from Korean historical books. J Geophys Res Space Phys 126:e2020JA028763. https://doi.org/10.1029/2020JA028763
Wang G, Yao S, Yu Y, Wei D, Di F, Bao X (2021b) Aurora sightings observed in Chinese history caused by CIRs or Great-Storm CMEs. Astrophys J 908:187. https://doi.org/10.3847/1538-4357/abd0fe
Willis DM, Stephenson FR (2000) Simultaneous auroral observations described in the historical records of China, Japan and Korea from ancient times to AD 1700. Ann Geophys 18:1–10. https://doi.org/10.1007/s00585-000-0001-6
Yau KKC, Francis RS, David MW (1995) A catalogue of auroral observations from China, Korea and Japan (193 B.C. - A.D. 170). Rutherford Appleton Laboratory Technical Reports: n. pag.
Zossi B, Hagay A, Mariano F, Ana GE (2021) Observed auroral ovals secular variation inferred from auroral boundary data. Geosciences 11(8):351. https://doi.org/10.3390/geosciences11080351

Publisher's Note

Springer Nature remains neutral with regard to jurisdictional claims in published maps and institutional affiliations.